Title
Intense vortex high-order harmonics generated from laser-ablated plume

Journal
Applied Physics Letters, 115(23)

ISSN
0003-6951

Authors
Singh, M
Fareed, MA
Laramée, A
et al.

Publication Date
2019-12-02

DOI
10.1063/1.5131289

Peer reviewed

Intense Vortex High-order Harmonics generated from Laser-ablated Plume

M. Singh,[1] M.A. Fareed,[1,2] A. Laramée,[1] E. Isgandarov,[1] and T. Ozaki [1,a)]
[1]Institut national de la recherche scientifique – Centre Energie Matériaux Telécommunications, 1650 Lionel-Boulet, Varennes, Québec J3X 1S2, Canada
[2]Lawrence Berkeley National Laboratory, University of California, Berkeley, California, 94720, USA
[a)]ozaki@emt.inrs.ca

Abstract

In this study, we demonstrate intense extreme-ultraviolet optical vortices generated using laser-ablation plume as the nonlinear medium. We used two types of plumes that are known to generate intense high-order harmonics for driving lasers with Gaussian beam profiles, but through different mechanisms, namely carbon (diatomic carbon molecules) and tin (resonance with autoionizing state). We find that the harmonic fluxes for diatomic carbon molecules are similar for Gaussian and vortex driving fields. However, for harmonics from the autoionizing state of tin (~26.3 eV), the enhancement factor of the resonant harmonic intensity decreases by ~50% when using the vortex driving field. The intense extreme-ultraviolet optical vortices demonstrated in this study will be useful for many applications including a new material characterization technique known as optical angular momentum dichroism as well as the spectroscopy of spin-forbidden electronic transitions.

High-order harmonic generation (HHG) from laser-ablated plumes (LAPs) has proven to be an excellent source of intense coherent extreme ultraviolet (XUV) and soft X-ray radiation.[1,2] We have previously demonstrated that graphite LAP could generate multi-μJ energy high-order harmonics (HOHs) over a relatively wide spectral range (17 eV to 26.3 eV).[3] Our recent study on the plasma spectroscopy of graphite LAP has revealed that these intense harmonics are generated from diatomic carbon molecules.[4] On the other hand, HHG from LAPs also has the potential to emit intense harmonics over a relatively narrow XUV spectral range by using resonances with autoionizing states (AIS) (for example, $\Delta\lambda_{\mathrm{FWHM}}$= ~ 0.75nm for the AIS of tin at 47.15 nm), a phenomenon known as resonant harmonic (RH) enhancement.[5,6,7] The HHG process from most laser-ablated materials can be explained by the three-step model.[8] According to this model, when an ultrafast laser pulse interacts with the laser-ablated atom or ion, an electron is tunnel ionized from the valence shell, accelerates away from the parent atom or ion by the applied field, and then recombines into the ground state upon reversal of the laser pulse electric field. On the other hand, the phenomenon of RH has been explained by the four-step model.[9] In this model, the first two steps are the same as the three-step model. However, in the third step, the electron in the continuum is scattered into the AIS of an atom or ion embedded in the continuum, which then experiences radiative decay into the initial ground state and emitting RH.[9] Emission of intense HOHs over a wide range of XUV spectrum is important for applications requiring intense attosecond pulses,[10,11] while narrowband intense RH finds a number of applications in the field of spectroscopy[12] and coherent nanoscale imaging.[13]

Light possessing optical angular momentum (OAM) due to twisted wavefront was pointed out more than two decades ago, and has fascinated researchers from a wide range of scientific community.[14] Laser beams carrying OAM, also known as optical vortices (OVs), contain a phase singularity at the center of the transverse intensity profile, resulting in a zero intensity in the center.[15] In the visible region of the electromagnetic spectrum, the OAM of OVs has long been utilized as an advantage in many applications, such as phase-contrast microscopy,[16] optical communication,[17] nanoparticle trapping,[18] quantum information,[19] and twisted nanostructure fabrication[20] to name a few.

In recent years, XUV-OVs have been successfully generated via HHG from noble gases using OV driving field.[21] Transfer of phase singularity from the fundamental laser beam into HOHs was successfully achieved even for highly nonlinear HHG processes. Interferometric measurements confirmed experimentally that the harmonic OAM is the product of the harmonic order and the OAM of the driving laser.[22] Attosecond pulse characterization using the RABBIT (reconstruction of attosecond beating by interference of two-photon transition) technique has shown OV harmonic phase-locking and hence the generation of attosecond XUV bursts.[23] These findings are truly a breakthrough, because many fascinating phenomena have been predicted as a result of the interaction of XUV-OVs with matter. These include a new material characterization technique known as OAM dichroism[24], high-resolution stimulated emission depletion (STED)-like microscopy without fluorophores[25], Skyrmionic defects with applications in the realization of nano-magnetic memory devices[26] and the observation of spin-forbidden transitions due to violation of selection rules during spectroscopic studies of light-matter interaction using OV driving field.[27,28]

Many such applications utilizing XUV-OVs require a substantial XUV flux. HHG from LAPs has been proven to be an extremely efficient process generating multi-μJ HOH energies using graphite LAP,[3] as well as near-μJ RH energy from tin LAP with ~10^{-4} conversion efficiency.[5]

Therefore, LAPs are extremely interesting candidates for the development of a tabletop source of high-flux XUV-OVs based on HHG. Such an efficient source could provide the high XUV flux required to study and develop many applications. The availability of high XUV flux could also allow single-shot data acquisition, which is extremely important for imaging applications where the incident XUV radiation could damage the sample to be studied, thus creating blurring effects due to long exposure time and hence resulting in less accurate morphological studies.[29] Single-shot data acquisition is also beneficial in ultrafast spectroscopic applications, eliminating measurement inaccuracies due to sample depletion and product accumulation caused by multiple laser shot irradiation.[30]

In this letter, we compare HOH obtained using a Gaussian and OV driving field for graphite as well as tin LAP, driven by an amplified Ti:sapphire laser. Graphite is used because of the emission of intense HOHs by diatomic carbon molecules present in the LAP via the three-step model. Tin LAP is studied due to the emission of intense RH close to ~26.3 eV. With diatomic carbon molecules, we find comparable HOH flux using both Gaussian and OV driving field in the energy region from 14 eV to 36 eV. For tin LAP using Gaussian driving field, we observe a RH enhancement factor of about 25 times compared to the neighboring harmonic. We demonstrate that tin LAP driven by OV laser beam also results in the generation of intense RH, but the enhancement factor is reduced by ~50% as compared to that observed using a Gaussian driving field.

The experimental scheme used to generate HOHs is shown in Fig.1. The experiment was performed on the 10 Hz beamline of the Advanced Laser Light Source (ALLS). The uncompressed Ti:sapphire laser pulse centered at 800 nm wavelength has a temporal duration of ~210 picoseconds. This laser beam is separated into two beams using a 30:70 beam splitter. The lower-energy laser beam is focussed onto the solid target surface with adjusted pulse energy, resulting in peak intensity of ~10^{10} W cm^{-2} at the focus, creating a plume over a diameter of ~ 170 μm. The higher-energy laser beam was compressed down to 60 fs, which is used to drive HHG. A 16-level spiral phase plate (SPP) manufactured by HOLO/OR Ltd. (Ness Ziona, Israel) was used to generate the OV driving field with topological charge 1. Fig.1 shows the image of the doughnut-shaped focal spot of the OV laser beam. The inner and outer diameter of the focal spot was measured to be ~45 μm and ~90 μm, respectively. The focal spot of the Gaussian laser beam was measured to be ~ 75 μm. For our comparative studies, the intensity of the Gaussian as well as the OV driving field at the focus was kept at ~ 2.2×10^{14} W cm^{-2}.

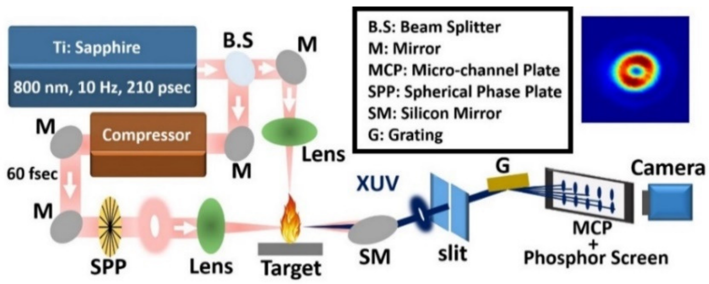

Fig. 1. Schematic diagram of the setup for the generation of high-order harmonics from laser-ablated plumes. Also shown is the doughnut-shaped focal spot of the vortex driving laser beam.

The target surface mounted onto an XYZ translation stage was placed inside a vacuum of ~10^{-5} Torr. To eliminate the co-propagating driving near-infrared laser pulses from the generated XUV pulses, a silicon mirror was installed at a Brewster angle, reflecting only the XUV radiation towards the XUV spectrometer. The spectrometer contained a fixed vertical slit, a cylindrical flat-field XUV grating (Hitachi, 1200 lines/mm) and a micro-channel plate (MCP) followed by a phosphor screen. The image of the HOHs detected onto the phosphor screen was captured by a 16-bit CMOS camera (model PCO-edge, PCO AG, Germany).

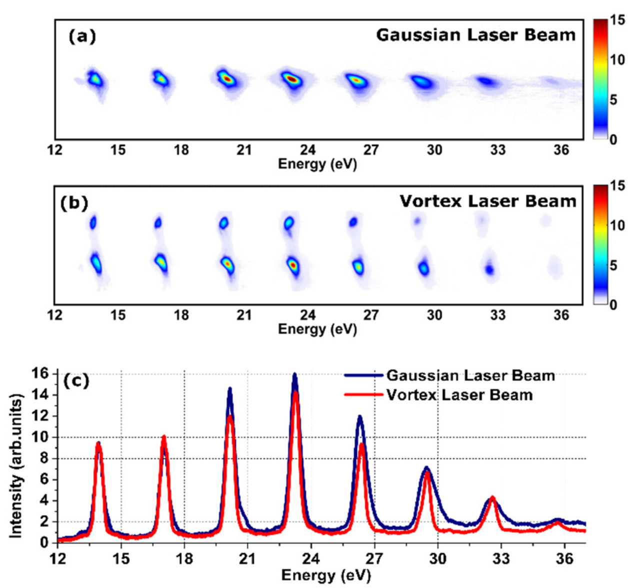

Fig. 2. Comparison of high-order harmonic intensity generated from graphite plume using Gaussian and vortex driving field. (a) The high-order harmonic spectra generated using a Gaussian driving field. (b) The double-lobe harmonic profile indicating vortex high-order harmonics. (c) Vertically integrated line plot showing a comparison of the high-order harmonic intensity obtained from the Gaussian and vortex driving field. The driving field intensity used to generate each spectrum is ~ 2.2×10^{14} W/cm^2.

The comparison of HOH flux obtained from diatomic carbon molecules using Gaussian and OV driving field is shown in Fig.2. The double-lobe harmonic profile in Fig.2(b) generated due to the presence of fixed vertical slit in the path of XUV-OV beam (which is expected to have a doughnut-shaped profile, as shown in Fig.1) clearly indicates the generation of OV-HOHs.[21] Interestingly, as can be seen from the line plot in Fig.2(c), we observed comparable HOH flux for the Gaussian and OV driving field.

The maximum XUV photon energy generated in this experiment is ~ 35 eV. According to the three-step model, the maximum photon energy emitted during the HHG process is the sum of the ionization potential (I_p) of the laser-ablated specie (atom, ion, or molecule) participating in HHG and the maximum kinetic energy of the returning tunnel ionized electron at the time of recombination into the ground state.[8] The ~35 eV cutoff is in agreement with our previous experiments with Gaussian driving field showing the dominant contribution of diatomic carbon molecules in the HHG from graphite LAP.[4] The same cutoff was observed with OV driving field, indicating HHG from diatomic carbon molecules is generating the XUV-OVs as well. Our previous investigations of HHG from diatomic carbon molecules demonstrate intense sub-100 eV XUV generation using an infrared driving field.[31] Therefore, our observation of comparable HOH flux with Gaussian and OV driving field suggests carbon molecules as a source of intense XUV-OVs over a wide spectral range with μJ harmonic energies in each harmonic order.[3]

Another important subject of investigation with HHG from LAP is the phenomenon of strong RH emission found in many materials.[32,33] The conversion efficiency of RH has been observed to be one to two-orders of magnitude higher than that of the neighboring harmonics generated by the three-step process. Therefore, here we study RH of tin for generating XUV-OVs.[5] Using Gaussian driving field, the RH emission close to 26.3 eV from tin LAP has been explained to be the result of multiphoton resonance of the driving laser photon with the high oscillator strength transition of Sn II from the AIS $4d^{10}\,5s^2\,5p\;^2P_{3/2}$ to the ground state $4d^9\,5s^2 5p^2\,(^1D)\;^2D_{5/2}$.[34] The comparison of the RH generated with Gaussian and OV driving field is shown in Fig.3. The 800 nm Ti:sapphire laser is approximately 17-photon resonant with the AIS transition of Sn II. By using a Gaussian driving field, the RH intensity obtained is approximately 25 times greater than the neighboring harmonics. However as clearly seen in Fig.3(c), the OV driving field reduces the

RH intensity by ~50% when compared with Gaussian driving field irradiation, while it has very little effect on the intensity of the other harmonics generated by the three-step model.

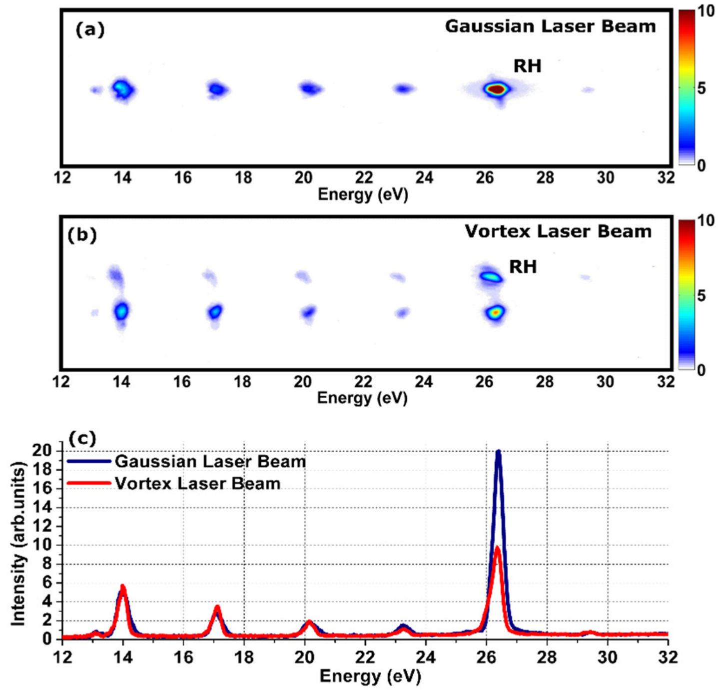

Fig. 3. Comparison of high-order harmonic intensity generated from tin plume using Gaussian and vortex driving field. (a) The high-order harmonic spectra generated using a Gaussian driving field. (b) The double-lobe harmonic profile indicating vortex high-order harmonics. (c) Vertically integrated line plot showing a comparison of the high-order harmonic intensity obtained from the Gaussian and vortex driving field. The weak harmonic present just below 14 eV is the second-order diffraction of XUV grating. The driving field intensity used to generate each spectrum is ~ 2.2×10^{14} W/cm^2.

This observation of similar three-step harmonic intensities for tin when using Gaussian and OV driving lasers is in agreement with our current results of HHG from diatomic carbon molecules. The ~50% reduction in the RH efficiency could be due to modifications in the characteristics of the laser-matter interactions with an OV driving field. Change in the state of motion of bound electron inside atoms due to the modified transition selection rules has already been reported using OV driving field; observation of spin-forbidden transitions being an important consequence.[27,28] Modified transition selection rules resulting in the reduction of oscillator strength of the transition from the AIS embedded in the continuum into the ground state with OV driving field excitation could be a possible explanation of the observed reduction in the RH intensity. Further spectroscopic investigations considering the dynamics of electronic transition involving AIS under OV driving fields are required for the true understanding of the phenomenon of reduction in RH intensity, which is outside the scope of this paper. Future aspect of our current experimental observations could involve the interferometric measurements of the phase of the RH and the three-step harmonics (i.e. the topological charge of the harmonics) generated using OV laser beam. This will give us another important parameter (apart from the RH suppression) to differentiate the behaviour of the RH and the three-step harmonics from LAPs driven with the OV laser beam.

In conclusion, we generate XUV-OV from diatomic carbon molecules in graphite LAP, with flux that is comparable to the XUV flux obtained through Gaussian driving field excitation. The graphite LAP has previously been reported to emit multi-μJ XUV harmonics, and our current observations suggest diatomic carbon molecules could be an intense source of XUV-OVs, finding applications that require high photon flux XUV-OVs. Further, using tin LAP driven with OV driving field, we still observe RH, but with an enhancement factor that is 50% of when a Gaussian driving field is used. This observation suggests the important implications of the modified laser-matter interaction in the presence of OV driving field onto the mechanism of RH generation, and hence motivates further investigations of the subject of RH in LAPs.

[1] R.A. Ganeev, M. Suzuki, M. Baba, and H. Kuroda, Appl. Phys. Lett. **86**, 131116 (2005).

[2] R.A. Ganeev, L.B.E. Bom, J.-C. Kieffer, M. Suzuki, H. Kuroda, and T. Ozaki, Phys. Rev. A **76**, 023831 (2007).

[3] L.B. Elouga. Bom, Y. Pertot, V.R. Bhardwaj, and T. Ozaki, Opt. Express **19**, 3077 (2011).

[4] M.A. Fareed, S. Mondal, Y. Pertot, and T. Ozaki, J. Phys. B **49**, 035604 (2016).

[5] M. Suzuki, M. Baba, R. Ganeev, H. Kuroda, and T. Ozaki, Opt. Lett. **31**, 3306 (2006).

[6] R.A. Ganeev, H. Singhal, P.A. Naik, V. Arora, U. Chakravarty, J.A. Chakera, R.A. Khan, I.A. Kulagin, P. V. Redkin, M. Raghuramaiah, and P.D. Gupta, Phys. Rev. A **74**, 063824 (2006).

[7] M.A. Fareed, V. V. Strelkov, N. Thiré, S. Mondal, B.E. Schmidt, F. Légaré, and T. Ozaki, Nat. Commun. **8**, 16061 (2017).

[8] P.B. Corkum, Phys. Rev. Lett. **71**, 1994 (1993).

[9] V. Strelkov, Phys. Rev. Lett. **104**, 123901 (2010).

[10] C. Winterfeldt, C. Spielmann, and G. Gerber, Rev. Mod. Phys. 80, **117** (2008).

[11] P.B. Corkum and F. Krausz, Nat. Phys. **3**, 381 (2007).

[12] S.L. Sorensen, O. Björneholm, I. Hjelte, T. Kihlgren, G. Öhrwall, S. Sundin, S. Svensson, S. Buil, D. Descamps, A. L'Huillier, J. Norin, and C.-G. Wahlström, J. Chem. Phys. **112**, 8038 (2000).

[13] M.D. Seaberg, D.E. Adams, E.L. Townsend, D.A. Raymondson, W.F. Schlotter, Y. Liu, C.S. Menoni, L. Rong, C.-C. Chen, J. Miao, H.C. Kapteyn, and M.M. Murnane, Opt. Express **19**, 22470 (2011).

[14] L. Allen, M.W. Beijersbergen, R.J.C. Spreeuw, and J.P. Woerdman, Phys. Rev. A **45**, 8185 (1992).

[15] A.G. White, C.P. Smith, N.R. Heckenberg, H. Rubinsztein-Dunlop, R. McDuff, C.O. Weiss, and C. Tamm, J. Mod. Opt. **38**, 2531 (1991).

[16] S. Fürhapter, A. Jesacher, S. Bernet, and M. Ritsch-Marte, Opt. Lett. **30**, 1953 (2005).

[17] J. Wang, J.-Y. Yang, I.M. Fazal, N. Ahmed, Y. Yan, H. Huang, Y. Ren, Y. Yue, S. Dolinar, M. Tur, and A.E. Willner, Nat. Photonics **6**, 488 (2012).

[18] D.G. Grier, Nature **424**, 810 (2003).

[19] J. Leach, B. Jack, J. Romero, A.K. Jha, A.M. Yao, S. Franke-Arnold, D.G. Ireland, R.W. Boyd, S.M. Barnett, and M.J. Padgett, Science **329**, 662 (2010).

[20] K. Toyoda, K. Miyamoto, N. Aoki, R. Morita, and T. Omatsu, Nano Lett. **12**, 3645 (2012).

[21] M. Zürch, C. Kern, P. Hansinger, A. Dreischuh, and C. Spielmann, Nat. Phys. **8**, 743 (2012).

[22] G. Gariepy, J. Leach, K.T. Kim, T.J. Hammond, E. Frumker, R.W. Boyd, and P.B. Corkum, Phys. Rev. Lett. **113**, 153901 (2014).

[23] R. Géneaux, A. Camper, T. Auguste, O. Gobert, J. Caillat, R. Taïeb, and T. Ruchon, Nat. Commun. **7**, 12583 (2016).

[24] M. van Veenendaal and I. McNulty, Phys. Rev. Lett. **98**, 157401 (2007).

[25] K.I. Willig, S.O. Rizzoli, V. Westphal, R. Jahn, and S.W. Hell, Nature **440**, 935 (2006).

[26] H. Fujita and M. Sato, Phys. Rev. B **95**, 054421 (2017).

[27] A. Picón, A. Benseny, J. Mompart, J.R. Vázquez de Aldana, L. Plaja, G.F. Calvo, and L. Roso, New J. Phys. **12**, 083053 (2010).

[28] C.T. Schmiegelow, J. Schulz, H. Kaufmann, T. Ruster, U.G. Poschinger, and F. Schmidt-Kaler, Nat. Commun. **7**, 12998 (2016).

[29] A. Ravasio, D. Gauthier, F.R.N.C. Maia, M. Billon, J.-P. Caumes, D. Garzella, M. Géléoc, O. Gobert, J.-F. Hergott, A.-M. Pena, H. Perez, B. Carré, E. Bourhis, J. Gierak, A. Madouri, D. Mailly, B. Schiedt, M. Fajardo, J. Gautier, P. Zeitoun, P.H. Bucksbaum, J. Hajdu, and H. Merdji, Phys. Rev. Lett. **103**, 028104 (2009).

[30] P.R. Poulin and K.A. Nelson, Science **313**, 1756 (2006).

[31] M.A. Fareed, N. Thiré, S. Mondal, B.E. Schmidt, F. Légaré, and T. Ozaki, Appl. Phys. Lett. **108**, 124104 (2016).

[32] R.A. Ganeev, *Resonance Enhancement in Laser-Produced Plasmas : Concepts and Applications* (Wiley, 2018).

[33] M.A. Fareed, V.V. Strelkov, M. Singh, N. Thiré, S. Mondal, B.E. Schmidt, F. Légaré, and T. Ozaki, Phys. Rev. Lett. **121**, 023201 (2018).

[34] G. Duffy, P. van Kampen, and P. Dunne, J. Phys. B **34**, 3171 (2001).